Control of Three Phase Inverters for Renewable Energy Systems under UnbalancedGrid Voltages

David J. Rincón[*], María A. Mantilla[*‡], Johann F. Petit[*], Gabriel Ordóñez[*] and Oscar Sierra[*]

[*]Grupo de Investigación en Sistemas de Energía Eléctrica
Escuela de Ingenierías Eléctrica, Electrónica y de Telecomunicaciones
Universidad Industrial de Santander
Bucaramanga, Colombia.

(davicos4@yahoo.com,marialem@uis.edu.co, jfpetit@uis.edu, gaby@uis.edu.co, oscarsierra21@hotmail.com)

[‡]Corresponding Author: María A. Mantilla; E-mail: marialem@uis.edu.co

Received: 03.02.2015 Accepted:19.03.2015

Abstract-This paper presents two control algorithms for grid-tied three-phase inverters for renewable energy systems under unbalanced grid voltages. The algorithms are focused on the quality of the injected currents, so they are used to inject balanced currents despite the voltage unbalances. Each algorithm is composed of three control loops: the reference signal generation, the reference signal synchronization and the curent controller. The first control loop generates the reference currents in order to regulate the active and the reactive powers delivered to the grid by the renewable energy system. The second loop is used to estimate the positive sequence component of the grid voltage. The last control loop generates the power inverter firing pulses in order to follow the reference current. In this paperare considered two algorithms, one algorithm in the *abc* coordinates and the other in the *dq0* coordinates. In both cases, it is considered a Kalman filter as the synchronization algorithm. The algorithms performance is evaluated by some simulations in PSIM and a comparative analysis is made between them. The results showed that the two algorithms present an outstanding performance in the injection of balanced currents with low total harmonic distortion despite the voltage unbalance. Also, the Kalman filter gets the desired estimation in less than a quarter of the grid period.

Keywords: inverters, power conditioning, renewable energy sources, unbalanced grid voltages.

1. Introduction

Nowadays, renewable energy sources are considered as a solution to meet the potential energy needs in the world. One motivation for the use of these energy sources is the exhaustion of the existing ones, like the fossil fuels. Another important reason is the global warming over the last years mainly due to greenhouse gases emissions[1]. In this way, the use of renewable energy systems as wind power and photovoltaic systems has grown fast over the last decade[2].

This kind of renewable energy sources has led to anincrease in the use of power inverters as an interface to connect the energy source to the utility network. A general diagram of a grid-tied inverter used for renewable systems applications is presented in Fig. 1[3]. In this paper, the DC input power and its control strategy are disregarded. A DC-AC converter known as power inverter is considered to transform the DC signal into an AC one. Also a connection filter and the inverter control system can be seen in Fig.1[4].The point where the system is connected to the grid is known as *Point of Common Coupling*(PCC).

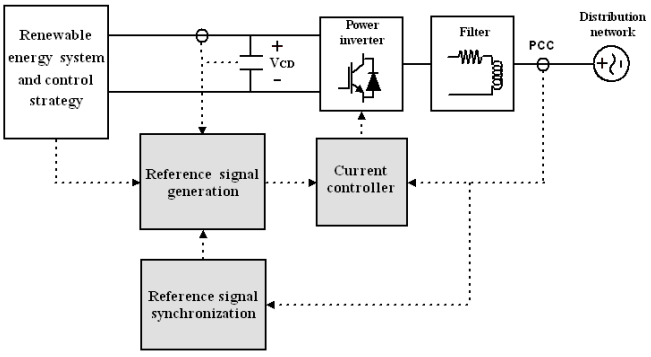

Fig. 1. General diagram of a grid-tied inverter for renewable systems applications.

The performance of the grid-tied system depends greatly of the control system, which is executed by three control loops:

- The reference signal generation
- The reference signal synchronization
- The current controller

The first two control loops are used to generate athree-phase reference current in order to deliver the desired active and reactive powers to the grid. The current controller is used togenerate the inverter firing pulses for tracking the reference signal.Furthermore, the injected current should follow some quality power specifications and requirements given by the corresponding standard by country[5]. So, these conditions have to be considered by the control system.

This paper is focused in the algorithms used to control thepower inverter when the voltages at the PCC are unbalanced. The unbalanced at the PCC voltage can produce harmonics and unbalances in the injected current when these conditions are not considered in the control algorithms[6]. These disturbancescould cause the non-compliance with the power quality standards[7]. Furthermore, the injection of unbalances currents can result in additional energy losses in the distribution system, additional heating and limitation of the line distribution capacityand unbalances in the system voltages.

In this way, different kind of strategies can be implemented to generate the inverter reference current under PCC unbalanced voltages, for example, the Instantaneous Active Reactive Control, the Instantaneously Controlled Positive Sequence, the Positive NegativeSequence Compensation, and the Balanced Positive Sequence Control, between others. These strategies differ from each other according to the quality of the current to be injected and possible oscillations in the resulting power[8].

This paper gives priority to the quality of the currents, so the reference signal generation algorithm is focused in obtain balanced currents despite the unbalances in the PCC voltage. Accordingly, this paper presents two reference signal generation algorithms, one in the *abc*coordinates and the other in the *dq0* coordinates. In both cases, it is considered a Kalman filter as the synchronization algorithm. This filter extract the positive sequence component of the PCC unbalanced voltage in order to syncronize the reference signal with this component and obtain balanced currents.

On the other hand, the inverter control is made by using a Dead-Beat controller when the reference current algorithm is in the *abc* coordinates and a Proportional-Integral regulator when the algorithm is in the *dq0* coordinates. Also, a Pulse Width Modulation (PWM) technique is used to generate the inverter firing pulses in both cases.

Accordingly, the organization of the paper is as follows. Section 2 shows the system model in both the *abc* coordinates and the *dq0* coordinates. In section 3, the control loops are described including the reference signal generation algorithms, the synchronization algorithm and the inverter controllers. The simulation results are presented in Section 4. Finally, the main conclusions of the work are shown.

2. System Model

The equivalent electric circuit of the grid-tied three-phase inverter is presented in Fig. 2. This equivalent is obtained based on the following assumptions[9].

- The input power source and its control strategy are disregarded, so the renewable energy source, the possible DC-DCand/or AC-DC converters andthe DC side capacitor aremodelled as an ideal DC voltage source VCD.
- The power semiconductors devicesof the power inverters are assumed as controlled ideal switches.
- The three-phase inverter is connected to the grid through a first order filter composed of an inductive element *L*. The resistor *R*represents the inductor resistance and it is disregarded for the controllers design.
- The equivalent electric network at the PCC is modeled by using a three-phase independent voltage source.
- The sampling frequency is 20 [kHz].

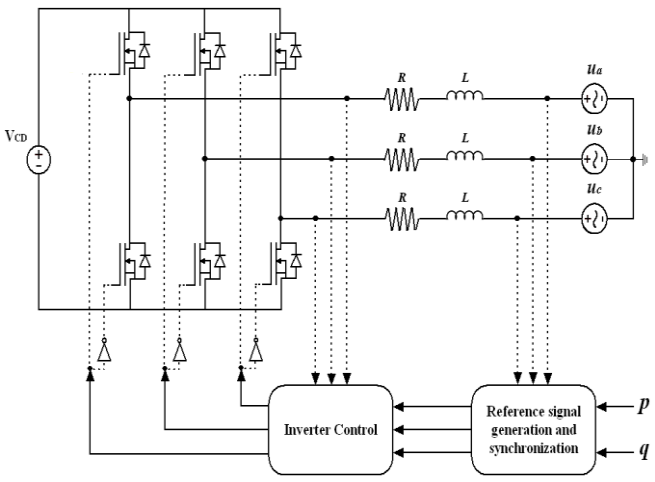

Fig. 2. Equivalent electric circuit of the grid-tied inverter.

2.1 System model in the abc coordinates

The model of the electric system can be found from the equivalent circuit presented in Fig.3, where u_a, u_b and $u_c$are the grid voltages at the PCC; u_{ainv}, u_{binv} and u_{cinv} are the output voltages at the power inverter, i_a, i_b and i_c are the injected currents and L is the connection coil. Taking into account the differential equations that describe the equivalent circuit, the system can be represented as shown in Eq. (1) [10].

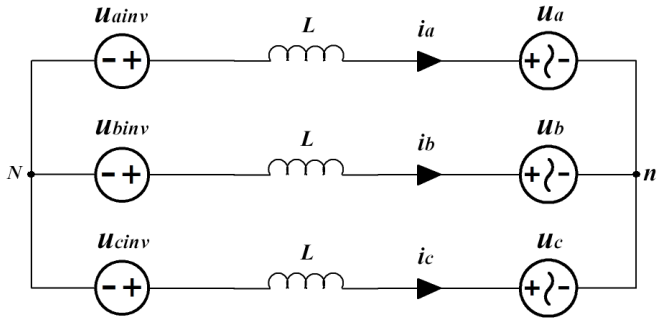

Fig. 3. Equivalent electric circuit.

$$\begin{bmatrix} u_{inva} \\ u_{invb} \\ u_{invc} \end{bmatrix} = \begin{bmatrix} 2/3 & -1/3 & -1/3 \\ -1/3 & 2/3 & -1/3 \\ -1/3 & -1/3 & 2/3 \end{bmatrix} \begin{bmatrix} L\frac{di_a}{dt} + u_a(t) \\ L\frac{di_b}{dt} + u_b(t) \\ L\frac{di_c}{dt} + u_c(t) \end{bmatrix} \tag{1}$$

2.2 System model in the dq0 coordinates

The model in the *dq0* coordinates can be found from the differential equations that describe the equivalent circuit in the *abc*coordinates and the Park transformation. The resulting model in the *dq* coordinates is shown in Eq. (2), where u_d and u_q are the grid voltages at the PCC in the *dq* coordinates, u_{dinv} and u_{qinv} are the inverter output voltages in the *dq* coordinates, i_d and i_q are the injected currents in those coordinates and ω is the grid frequency [11]. In this case, the zero sequence current component is neglected because it is considered a three-phase three-wire system as shown in Fig.2.

$$\begin{bmatrix} u_{dinv} \\ u_{qinv} \end{bmatrix} = L\frac{d}{dt}\begin{bmatrix} i_d \\ i_q \end{bmatrix} + L\omega\begin{bmatrix} -i_q \\ i_d \end{bmatrix} + \begin{bmatrix} u_d \\ u_q \end{bmatrix} \tag{2}$$

3. Control Algorithms

The control algorithms are shown according to the following classification: the reference signal generation techniques, the synchronization algorithm and the current controllers.

3.1 Reference signals generation

When the voltages are unbalanced in the PCC, the system can be controlled in different ways according to the quality of the current and the characteristics of the power to be injected[12]. This paper gives priority to the quality of the currents, so the signal reference generation algorithm is focused on getting balanced reference currents without harmonic distortion.

The unbalanced three-phase voltage at the PCC can be decomposed into the sum of a positive sequence u_k^+, a negative sequence u_k^- and a zero sequence u_k^0, as follows[13]:

$$u_k(t) = u_k^+(t) + u_k^-(t) + u_k^0(t) \therefore k = a,b,c \tag{3}$$

These voltages can be expressed according to equation (4), where u^0, u^+ and u^- are the amplitudes and θ^0, θ^+ and θ^- the angles for the zero sequence, the positive sequence and the negative sequence, respectively[13].

$$\begin{aligned} u_a &= u^0\cos(\theta^0) + u^+\cos(\theta^+) + u^-\cos(\theta^-) \\ u_b &= u^0\cos(\theta^0) + u^+\cos(\theta^+ - \frac{2\pi}{3}) + u^-\cos(\theta^- + \frac{2\pi}{3}) \\ u_c &= u^0\cos(\theta^0) + u^+\cos(\theta^+ + \frac{2\pi}{3}) + u^-\cos(\theta^- - \frac{2\pi}{3}) \end{aligned} \tag{4}$$

Furthermore, these symmetrical components can be represented in the *αβ0* coordinates and the *dq0* coordinates according to equations (5) and (6), respectively.

$$\begin{bmatrix} u_\alpha \\ u_\beta \\ u_0 \end{bmatrix} = \begin{bmatrix} u_\alpha^+ + u_\alpha^- \\ u_\beta^+ + u_\beta^- \\ u_0 \end{bmatrix} \tag{5}$$

$$\begin{bmatrix} u_d \\ u_q \\ u_0 \end{bmatrix} = \begin{bmatrix} u_d^+ + u_d^- \\ u_q^+ + u_q^- \\ u_0 \end{bmatrix} \tag{6}$$

- The currents can also be decomposed into symmetrical components just as the voltage.
- The zero sequence current component is disregarded because it is considered a three-phase three-wire system.
- The control algorithms seek to generate a balanced current of positive sequence as shown in equation Eq. (7) for the three-phases.

$$\begin{aligned} i_a &= i^+ \cos(\theta^+) \\ i_b &= i^+ \cos(\theta^+ - 120^\circ) \\ i_c &= i^+ \cos(\theta^+ + 120^\circ) \end{aligned} \quad (7)$$

These components in the *αβ0* coordinates and the *dq0* coordinates are given Eq. (8) and Eq. (9) respectively.

$$\begin{bmatrix} i_\alpha \\ i_\beta \end{bmatrix} = \begin{bmatrix} i_\alpha^+ \\ i_\beta^+ \end{bmatrix} \quad (8)$$

$$\begin{bmatrix} i_d \\ i_q \end{bmatrix} = \begin{bmatrix} i_d^+ \\ i_q^+ \end{bmatrix} \quad (9)$$

Considering these balanced reference currents, the injected active power is defined as the sum of two components[14], an average power $\bar{p}$ and an oscillatory power $\tilde{p}$:

$$p = \bar{p} + \tilde{p} \quad (10)$$

Where the average active power is given by equation (11).

$$\bar{p} = u_d^+ i_d^+ + u_q^+ i_q^+ \quad (11)$$

The oscillatory component of the active power $\tilde{p}$ is given by the interaction of the negative sequence component of the PCC voltage and the positive sequence component of the injected current, in this case $u_d^- i_d^+$ and $u_q^- i_q^+$. Similarly, this analysis is made for the reactive power:

$$q = \bar{q} + \tilde{q} \quad (12)$$

Where:

$$\bar{q} = u_q^+ i_d^+ - u_d^+ i_q^+ \quad (13)$$

The oscillatory component of the reactive power $\tilde{q}$ is given by the interaction of the negative sequence component of the PCC voltage and the positive sequence component of the injected current, in this case $u_d^- i_q^+$ and $u_q^- i_d^+$.

3.1.1 Reference currents in the dq0 coordinates

In this coordinates, equations can be simplified if the system is synchronized with the positive sequence component of the PCC voltage[15], because the quadrature component of this voltage(u_q^+) is zero. Therefore, the reference currents may be expressed as[8]:

$$i_d^+ = \frac{\bar{p}}{u_d^+} \quad (14)$$

$$i_q^+ = -\frac{\bar{q}}{u_d^+} \quad (15)$$

3.1.2 Reference currents in the abc coordinates

The algorithm is based on the decomposition of the currents into two signals, one component only provides active power (subscript p) and the other component only provides reactive power (subscript q). In this way, the currents for each phase are represented as follows:

$$\begin{bmatrix} i_a^+ \\ i_b^+ \\ i_c^+ \end{bmatrix} = \begin{bmatrix} i_{ap}^+ \\ i_{bp}^+ \\ i_{cp}^+ \end{bmatrix} + \begin{bmatrix} i_{aq}^+ \\ i_{bq}^+ \\ i_{cq}^+ \end{bmatrix} \quad (16)$$

In order to find the two components of the currents, firstly the reference currents in the *αβ0*coordinates are expressed as a function of the average active power and the average reactive power according to equation (15).

$$\begin{bmatrix} i_\alpha^+ \\ i_\beta^+ \end{bmatrix} = \frac{1}{u_\alpha^{+2} + u_\beta^{+2}} \begin{bmatrix} u_\alpha^+ & u_\beta^+ \\ u_\beta^+ & -u_\alpha^+ \end{bmatrix} \begin{bmatrix} \bar{p} \\ \bar{q} \end{bmatrix} \quad (17)$$

Then, equation (18) is obtained by using the inverse of the Clark transformation.

$$\begin{bmatrix} i_a^+ \\ i_b^+ \\ i_c^+ \end{bmatrix} = \sqrt{\frac{2}{3}} \begin{bmatrix} 1 & 0 \\ -\frac{1}{2} & \frac{\sqrt{3}}{2} \\ -\frac{1}{2} & -\frac{\sqrt{3}}{2} \end{bmatrix} \frac{1}{u_\alpha^{+2} + u_\beta^{+2}} \begin{bmatrix} u_\alpha^+ & u_\beta^+ \\ u_\beta^+ & -u_\alpha^+ \end{bmatrix} \begin{bmatrix} \bar{p} \\ \bar{q} \end{bmatrix} \quad (18)$$

Finally, the components of the currents are separated and the equivalent voltages in the *abc* coordinates are replaced:

$$\begin{bmatrix} i_{ap}^+ \\ i_{bp}^+ \\ i_{cp}^+ \end{bmatrix} = \frac{\bar{p}/3}{u_a^{+2} + u_b^{+2} + u_c^{+2}} \begin{bmatrix} 2u_a^+ - u_b^+ - u_c^+ \\ -u_a^+ + 2u_b^+ - u_c^+ \\ -u_a^+ - u_b^+ + 2u_c^+ \end{bmatrix} \quad (19)$$

$$\begin{bmatrix} i_{aq}^+ \\ i_{bq}^+ \\ i_{cq}^+ \end{bmatrix} = \frac{\bar{q}/\sqrt{3}}{u_a^{+2} + u_b^{+2} + u_c^{+2}} \begin{bmatrix} 0 + u_b^+ - u_c^+ \\ -u_a^+ + 0 + u_c^+ \\ u_a^+ - u_b^+ + 0 \end{bmatrix} \quad (20)$$

3.2 Reference signals synchronization: The Kalman filter

According to the reference signal generation algorithms, it is needed a previous estimation of the positive sequence component of the PCC voltage in order to synchronize the reference currents and guarantee the injection of balanced currents. In this way, this previous estimation is made by using a kalman filter.

The Kalman filter is a recursive algorithm that can estimate the states of a dynamic system with Gaussian white noise by using measures related to the states. These measures can also be contaminated with such kind of noise[13].

The Kalman filter is based on the system model and the relationship between the measures and the states. Once the model and this relationship are established, the filter only needs the measures at time n and the value of the states at time n-1, in order to estimate the states at time n and predict the states for n+1[16].

The basic equations used to implement the algorithm are: the state equation and the measurement equation, which are presented below:

State equation:

$$\boldsymbol{X}(\mathrm{n}+1)=\boldsymbol{A}(\mathrm{n})\boldsymbol{X}(\mathrm{n})+\boldsymbol{U}_1(\mathrm{n}) \tag{21}$$

Where $X(\mathrm{n})$ is the states vector at n, $X(\mathrm{n}+1)$ is the states vector at n+1, $A(\mathrm{n})$ is the states transition matrix that relates the states at n+1 with the states at n. The last term $U_1(\mathrm{n})$ corresponds to the white noise due to random variations of the states.

Measurement equation:

$$\boldsymbol{Z}(n)=\boldsymbol{H}(n)\boldsymbol{X}(n)+\boldsymbol{U}_2(n) \tag{22}$$

Where $Z(\mathrm{n})$ represents the vector of the measured signals, $H(\mathrm{n})$ is the measurements matrix and $\boldsymbol{U}_2(n)$ represents the random error due to the measurement and it is uncorrelated with the noise $\boldsymbol{U}_1(n)$.

Fig.4 shows he iterative process of the Kalman algorithm, where: $P(\mathrm{n})$ is the error covariance matrix, $K(\mathrm{n})$ is the Kalman gain, $\boldsymbol{I}$is the identity matrix, $R(\mathrm{n})$ is the covariance matrix associated with the noise vector $U_1(\mathrm{n})$ whose value is given by $R(\mathrm{n})=\sigma_r^2 I$; and $Q(\mathrm{n})$ is the covariance matrix associated with the noise vector $U_2(\mathrm{n})$ whose value is given by $Q(\mathrm{n})=\sigma_q^2 I$.

The covariances σ_r and σ_q must be determined for an optimal performance of the algorithm according to the application.

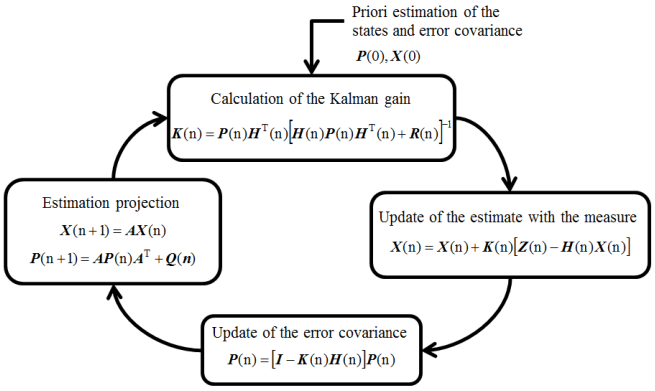

Fig. 4. Kalman algorithm.

In this application, the Kalman filter is implemented in order to estimate the positive sequence component of the PCC voltage. For this, the state vector is selected as[13]:

$$\begin{bmatrix} x_1 \\ x_2 \\ x_3 \\ x_4 \end{bmatrix}=\begin{bmatrix} u^+\cos(\theta^+) \\ u^+\sin(\theta^+) \\ u^-\cos(\theta^-) \\ u^-\sin(\theta^-) \end{bmatrix} \tag{23}$$

According to the state vector, the state equation and the measurement equation are given by Eq. (24) and Eq. (25) respectively.

$$\begin{bmatrix} \boldsymbol{x}_1(n+1) \\ \boldsymbol{x}_2(n+1) \\ \boldsymbol{x}_3(n+1) \\ \boldsymbol{x}_4(n+1) \end{bmatrix}=\begin{bmatrix} \boldsymbol{A} & 0 \\ 0 & \boldsymbol{A} \end{bmatrix}\begin{bmatrix} \boldsymbol{x}_1(n) \\ \boldsymbol{x}_2(n) \\ \boldsymbol{x}_3(n) \\ \boldsymbol{x}_4(n) \end{bmatrix}+\boldsymbol{U}_1(\boldsymbol{n}) \tag{24}$$

Where:

$$A=\begin{bmatrix} \cos(\omega_f T_s) & -\sin(\omega_f T_s) \\ \sin(\omega_f T_s) & \cos(\omega_f T_s) \end{bmatrix}$$

$$\begin{bmatrix} \boldsymbol{u}_{ab}(\mathrm{n}) \\ \boldsymbol{u}_{bc}(\mathrm{n}) \end{bmatrix}=\begin{bmatrix} \frac{3}{2} & -\frac{\sqrt{3}}{2} & \frac{3}{2} & -\frac{\sqrt{3}}{2} \\ 0 & \sqrt{3} & 0 & \sqrt{3} \end{bmatrix}\begin{bmatrix} \boldsymbol{x}_1(\mathrm{n}) \\ \boldsymbol{x}_2(\mathrm{n}) \\ \boldsymbol{x}_3(\mathrm{n}) \\ \boldsymbol{x}_4(\mathrm{n}) \end{bmatrix}+\boldsymbol{U}_2(\mathrm{n}) \tag{25}$$

Finally, the positive sequence voltages can be obtained from the states, as shown below:

$$\begin{bmatrix} u_a^+ \\ u_b^+ \\ u_c^+ \end{bmatrix} = \begin{bmatrix} 1 & 0 \\ -1/2 & \sqrt{3}/2 \\ -1/2 & -\sqrt{3}/2 \end{bmatrix} \begin{bmatrix} x_1 \\ x_2 \end{bmatrix} \quad (26)$$

The positive sequence amplitude u^+ can be obtained from the states x_1 and x_2, as shown in Eq. (27).

$$u^+ = \sqrt{x_1^2 + x_2^2} \quad (27)$$

In the *dq0* coordinates, the positive sequence component can be obtained by using equation (28).

$$\begin{bmatrix} u_d^+ \\ u_q^+ \end{bmatrix} = \sqrt{\frac{2}{3}} \begin{bmatrix} y_1 & -\frac{1}{2}y_1 + \frac{\sqrt{3}}{2}y_2 & -\frac{1}{2}y_1 - \frac{\sqrt{3}}{2}y_2 \\ -y_2 & \frac{\sqrt{3}}{2}y_1 + \frac{1}{2}y_2 & -\frac{\sqrt{3}}{2}y_1 + \frac{1}{2}y_2 \end{bmatrix} \begin{bmatrix} u_a^+ \\ u_b^+ \\ u_c^+ \end{bmatrix} \quad (28)$$

Where $y_1 = \cos(\theta^+)$ and $y_2 = \sin(\theta^+)$.

3.3 Current controllers

The current controllers are used to determine the reference voltage signals at the inverter AC side in order to follow the reference currents. Subsequently, the reference voltage signals are synthesized by using a Pulse Witdth Modulation (PWM) technique in order to generate the firing pulses.

3.3.1 Predictive controller (Dead-Beat)

This control technique predicts the inverter output voltage by using the model of the system in order to reach the reference currents by the end of the next modulation period[10].

The voltage signals are determined from the discrete model of the system in the *abc* coordinates. This model is calculated by using the bilinear transformation and the model presented in equation (1). The resulting algorithm isshown in equation (29).

$$\begin{bmatrix} u_{inva} \\ u_{invb} \\ u_{invc} \end{bmatrix} = \begin{bmatrix} 2/3 & -1/3 & -1/3 \\ -1/3 & 2/3 & -1/3 \\ -1/3 & -1/3 & 2/3 \end{bmatrix} + \begin{bmatrix} \frac{L}{T_s}e_a + u_a(\mathrm{n}) \\ \frac{L}{T_s}e_b + u_b(\mathrm{n}) \\ \frac{L}{T_s}e_c + u_c(\mathrm{n}) \end{bmatrix} \quad (29)$$

Where $e_k = i_k^+(\mathrm{n}) - i_{kinv}(\mathrm{n})$ for $k = a,b,c$; $i_k^+(\mathrm{n})$ and $i_{kinv}(\mathrm{n})$ are the reference current and the injected current for the *k* phase, respectively.

3.3.2 Proportional-integral control in dq0 coordinates (PI-dq0)

This controller is used to estimate the derivatives of the currents in the *dq0* coordinates as a function of the injected currents errors, as shown in equations (30) and (31)[17].

$$\begin{bmatrix} D_1(t) \\ D_2(t) \end{bmatrix} = \begin{bmatrix} L\frac{di_d(t)}{dt} \\ L\frac{di_q(t)}{dt} \end{bmatrix} \quad (30)$$

$$D_k(t) = k_{pk}e_k(t) + \frac{k_{pk}}{T_{ik}}\int e_k(t)dt \therefore k = 1,2 \quad (31)$$

Where the current errors in the*dq* coordinates are given by: $e_1(t) = i_d^+(t) - i_{dinv}(t)$ and $e_2(t) = i_q^+(t) - i_{qinv}(t)$.

Equation is discretized in order to obtain:

$$D_k(\mathrm{n}) = k_{pk}[e_k(\mathrm{n}) - e_k(\mathrm{n}-1)] + \frac{k_{pk}}{T_{ik}}e_k(\mathrm{n}) + D_k(\mathrm{n}\text{-}1) \therefore k = 1,2 \quad (32)$$

Once these derivatives are estimated, equation (2) is used to determine the output voltage of the inverter in the *dq* coordinates. Finally, the inverses of the Clark and Park transformations are used to find the voltages in the *abc*, sotheycanbesynthesizedbythePWMtechnique.

4. Simulations and Results

The algorithms performance was evaluated by simulations in the software PSIM and the results were compared based on the following parameters: the Total Harmonic Distortion (THD) of the injected currents, the Mean Square Error (MSE) and the Instantaneous Maximum Error (IME) in steady-state in the injected currents; and the MSE in the powers.

The voltages considered at the PCC are shown in Fig.5.Eq. (33) and Eq. (34) show the voltagesfor$0 \le t < 0.05$ [s] and $0.05 \le t < 1$ [s] respectively, with $u^+ = 120\sqrt{2}$ [V], $u^- = 12\sqrt{2}$ [V], $u^0 = 1.2\sqrt{2}$ [V], $\theta^+ = \theta^- = \theta^0 = 120\pi t$ [rad]. It is noticed that there is a change in the phase of the PCC voltage.Also, a negative and a zero sequence components are includedin the voltage since *t=0.05*[s].

$$\begin{bmatrix} u_a \\ u_b \\ u_c \end{bmatrix} = \begin{bmatrix} u^+ \sin(\theta) \\ u^+ \sin(\theta + \frac{2\pi}{3}) \\ u^+ \sin(\theta - \frac{2\pi}{3}) \end{bmatrix} \quad (33)$$

$$\begin{bmatrix} u_a \\ u_b \\ u_c \end{bmatrix} = \begin{bmatrix} u^+ \sin(\theta + \frac{\pi}{4}) + u^- \sin(\theta + \frac{\pi}{4}) + u^0 \sin(\theta + \frac{\pi}{4}) \\ u^+ \sin(\theta - \frac{5\pi}{12}) + u^- \sin(\theta + \frac{11\pi}{12}) + u^0 \sin(\theta + \frac{\pi}{4}) \\ u^+ \sin(\theta + \frac{11\pi}{12}) + u^- \sin(\theta - \frac{5\pi}{12}) + u^0 \sin(\theta + \frac{\pi}{4}) \end{bmatrix} \quad (34)$$

The simulation parameters are presented in Table 1. In this case, the average values for the active and reactive powers were chosen in order to consider a 0.8 leading power factor.

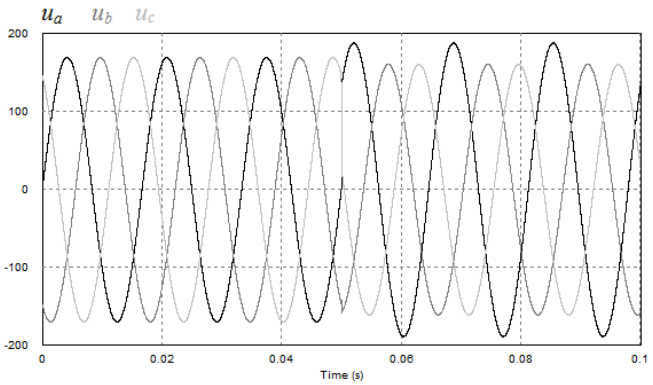

Fig. 5. Voltages at the PCC.

4.1 Synchronization algorithm results

The positive sequence component of the PCC voltage and its estimation by using the Kalman filter are shown in Fig. 6. As can be seen, the Kalman filters extracts accurately this component even under negative and zero sequence unbalances. Also, the response time of the filter is almost a quarter of the grid period.

Table 1. Simulation parameters

Variable	Value
$\bar{p}_{ref}$	2000[W]
$\bar{q}_{ref}$	-1500 [VAR]
L	20 [mH]
f_{Grid}	60 [H]
$f_{sampling}$	20 [kH]
σ_r	$1*10^{-5}$
σ_q	$3*10^{-8}$
PWM peak to peak value	519.61
k_{p1}, k_{p2}	300
T_{i1}, T_{i2}	50000
V_{dc}	450 [V]

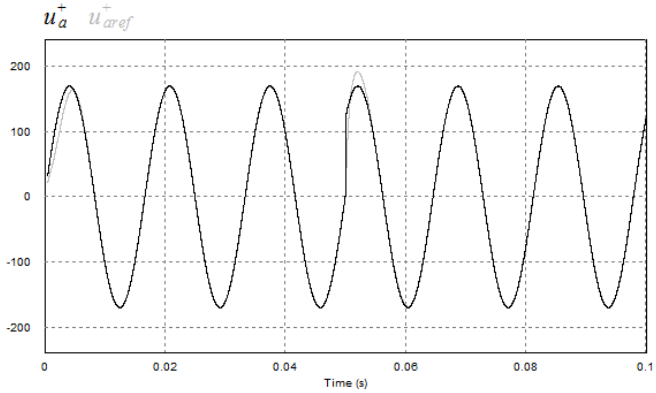

Fig. 6. Positive sequence component of the PCC voltage (black line) and its estimation (grey line).

4.2 Results: algorithm in the abc coordinates

The currents injected to the grid by using the referece signal generation algorithm in the *abc* coordinates and the Dead-beat controller are shown in Fig 7.

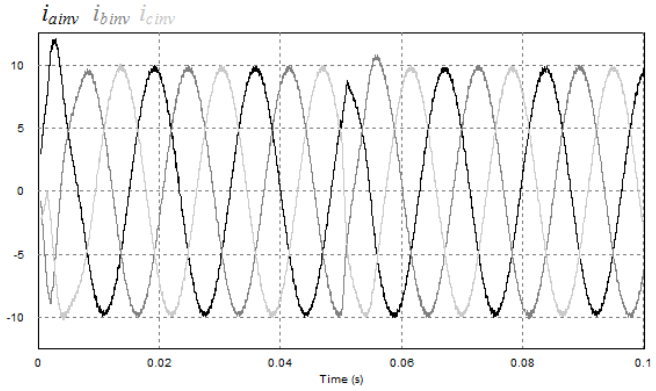

Fig. 7. Currents injected to the grid by using *abc* – Dead-Beat controllers.

Table 2. shows the rms values of the reference currents, the rms values of the injected currents and the THD when the grid voltages are ideal, likewise Table 3. shows the same parameters but when the grid voltages are unbalanced.

Table 2. Currents injected to the grid using *abc* – Dead-Beat controllers with idealgrid voltages.

i_{ref} (A_{rms})		i_{inv} (A_{rms})		THD	
i_a	6.95	i_{ainv}	6.89	i_{ainv}	1.60%
i_b	6.95	i_{binv}	6.89	i_{binv}	1.37%
i_c	6.94	i_{cinv}	6.88	i_{cinv}	1.43%

Table 3. Currents injected to the grid using *abc* – Dead-Beat controllers with unbalaced grid voltages.

i_{ref} (A_{rms})		i_{inv} (A_{rms})		THD	
i_a	6.94	i_{ainv}	6.86	i_{ainv}	1.53%
i_b	6.94	i_{binv}	6.92	i_{binv}	1.50%
i_c	6.94	i_{cinv}	6.88	i_{cinv}	1.69%

It can be observed that the THD of the injected currents is very low, either with ideal or unbalanced voltages. Likewise, the tracking of the injected currents with respect to the reference currents is very good in both cases.

Fig.8 presents the active and the reactive powers injected to the grid. As can be observed, after *t=0.05* [s] the powers have an oscillatory component due to the interaction of the negative sequence component of the PCC voltage and the positive sequence component of the injected currents. Also, there is a ripple in the injected powers due to the switching operation of the power inverter. Notice that the overshoot in the reactive power is generatedby thechange in the phase of the PCC voltageat *t=0.05* [s]. This transient response is due to the delay of the Kalman filter (response time) in the estimation of the positive sequence component of the PCC voltages, as can be seen in Fig. 6.

Table 4. shows the average value of the active and reactive powers injected to the grid with both ideal and unbalanced voltages at the PCC. As can be seen, it is obtained small errors even under unbalanced voltages, so the controllers achive the proposed goals.

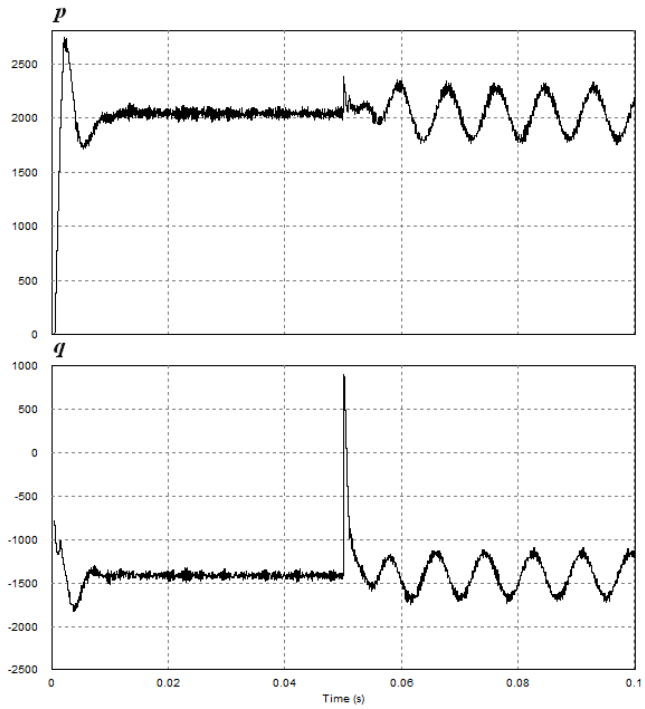

Fig. 8. Active and reactive powers by using the *abc* – Dead-Beat controller

Table 4. Injected powers to the grid using *abc* – Dead-Beat controllers.

	$\overline{p}$ (W)	e_p	$\overline{q}$ (VAR)	e_q
U_{ideal}	2044	2.2%	-1411	5.93%
$U_{unbalanced}$	2040	2%	-1412	5.86%

4.3 Results: algorithm in the dq0 coordinates

The three-phase injected currents by using the reference signal algorithm in the the *dq0* coordinates and the PI-*dq0* controller are shown in Fig. 9.

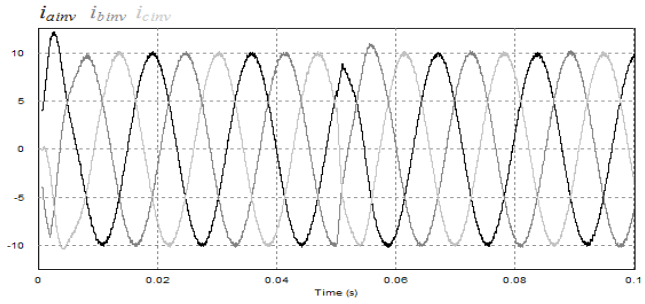

Fig. 9. Currents injected to the grid by using the *dq0* - PI*dq0* controller.

Table 5. shows the rms values of the reference currents, the rms values of the injected currents and the THD when the grid voltages are ideal, likewise Table 6. shows the same parameters but when the grid voltages are unbalanced.

Table 5. Currents injected to the grid using the *dq0* - PI*dq0* controller with idealgrid voltages.

i_{ref} (A_{rms})		i_{inv} (A_{rms})		**THD**	
i_a	6.94	i_{ainv}	7.01	i_{ainv}	1.29%
i_b	6.94	i_{binv}	7.01	i_{binv}	1.37%
i_c	6.94	i_{cinv}	7.01	i_{cinv}	1.38%

Table 6. Currents injected to the grid using the *dq0* - PI*dq0* controller with unbalanced grid voltages.

i_{ref} (A_{rms})		i_{inv} (A_{rms})		**THD**	
i_a	6.94	i_{ainv}	6.96	i_{ainv}	1.33%
i_b	6.94	i_{binv}	7.05	i_{binv}	1.39%
i_c	6.94	i_{cinv}	7.01	i_{cinv}	1.32%

Fig.10 shows the active and the reactive powers injected to the grid by using the algorithms in the *dq0* coordinates. As can be observed, after *t=0.05* [s] the powers have an oscillatory component and a small ripple as it was expected.

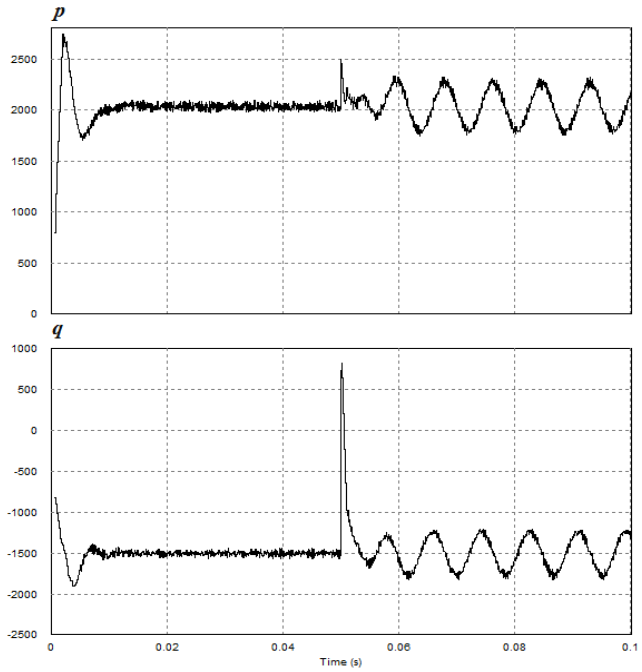

Fig. 10. Active and reactive powers by using *dq0* – PI*dq0*.

The average value of the active and reactive powers injected to the grid with both ideal and unbalanced voltages at the PCC by using the algorithm in the *dq0* coordinates is presented in Table 7. As can be seen, it is obtained smaller errors than those obtaing with the algorithm in the *abc* coordinates.

Table 7. Injected powers to the grid by using the *dq0* - PI*dq0* controller.

	$\bar{p}$ (W)	ep	$\bar{q}$ (VAR)	eq
Uideal	2034	1.7%	-1502	0.13%
Uunbalanced	2031	1.55%	-1501	0.06%

4.4 Comparison results

Finally, Table 8. presents a comparison between theperformance of the controllers in steady state when the grid voltages are ideal. The comparison isbased on the parameters mentioned before. Also, Table 9. shows the same comparison but with unbalanced voltages in the PCC.

Table 8. Comparison results considering ideal voltages.

	Ref. abc - Dead-Beat			***Ref. dq0 – Pidq0***		
	i_{ainv}	i_{binv}	i_{cinv}	i_{ainv}	i_{binv}	i_{cinv}
THD	1.60%	1.37%	1.43%	1.29%	1.37%	1.38%
IME	8.22%	7.39%	6.40%	5.86%	5.80%	5.84%
MSE	2.65%	2.65%	2.58%	2.10%	2.15%	2.22%

Table 9. Comparison results with unbalanced voltages

	Ref. abc - Dead-Beat			***Ref. dq0 – Pidq0***		
	i_{ainv}	i_{binv}	i_{cinv}	i_{ainv}	i_{binv}	i_{cinv}
THD	1.53%	1.60%	1.69%	1.33%	1.39%	1.32%
IME	7.73%	8.22%	8.29%	5.25%	6.35%	5.23%
MSE	2.60%	2.54%	3.18%	2.14%	2.59%	1.70%

As can be observed in Table 8. and Table 9., the injected currents present low harmonic distortion (THD < 5%) by using either of the two algorithms. Also, these currents are balanced despite the voltage unbalances at the PCC, so the control algorithms achive the proposed goals. According to the MSE and IME values, the performance of both algorithms is very similar. The biggest different between the algorithms is that the one in the *dq0* coordinates requires the transformation of the electrical signals from the *abc* to *dq0* coordinates, and vice versa.

5. Conclusions

This paper presented two algorithms used to control the active and reactive powers in grid-tied three-phase inverters for renewable energy sources applications. The algorithms were focus in the quality of the injected currents under PCC unbalanced voltages, one algorithm in the *abc* coordinates and the other in the *dq0* coordinates.Both algorithms were synchronized by a Kalman filter. This filter was used to estimate the positive sequence component of the PCC voltages and guarantee the injection of balanced and sinusoidal currents. The simulations results showed that the two algorithms present an outstanding performance in the injection of balanced currents with low total harmonic distortion despite the voltage unbalances. However, the algorithm implemented in the *dq0* coordinates showed smaller power error than the algorithm in the *abc* coordinates. Furthermore, both algorithms follows the average value of the active and reactive reference powers, however the injection of balanced currents leads to oscillations in the active and reactive instantaneous powers.

References

[1] R. Pode and B. Diouf, Solar Lighting, 1st ed, Springer, 2011, pp.68-73.

[2] A. Martí and A. Luque, Next generation photovoltaics: High efficiency through full spectrum utilization, 1st ed, Institute of Physics Publishing, 2004.

[3] R. Mastromauro, M. Liserre, and A. Dell'Aquila, "Control Issues in Single-Stage Photovoltaic Systems:MPPT, Current and Voltage Control",IEEE Transactions on Industrial Informatics, vol. 8,No. 2, pp. 241 -254, May 2012.

[4] M. Schonardie, A. Ruseler, R. Coelho, and D. Martins, "Three-phase grid-connected PV system with active and reactive power control using dq0 transformation", 2010 9th IEEE/IAS InternationalConference onIndustry Applications (INDUSCON), pp. 1-6, Nov. 2010.

[5] IEEEStandard 154-2003, IEEE Recommended Practice for Interconnecting Distributed Resources with Electric Power Systems,The Institute of Electrical and Electronics Engineers, 2003.

[6] L. Fan, Z. Miao, and A. Domijan, "Impact of unbalanced grid conditions on PV systems",2010 IEEE Power and Energy Society General Meeting, pp. 1-6, July 2010.

[7] S. Xian-wen, W. Yue, and W. Zhao-an, "Dual reference frame scheme for distributed generation grid-connected inverter under unbalanced grid voltage conditions",IEEE Power Electronics Specialists Conference(PESC), pp. 4552-4555, June 2008.

[8] P. Rodriguez, A. Timbus, R. Teodorescu, M. Liserre, and F. Blaabjerg, "Flexible Active Power Control of Distributed Power Generation Systems During Grid Faults," IEEE Transactions on Industrial Electronics, vol. 54,No. 5, pp. 2583-2592, Oct. 2007.

[9] M. Mantilla, D. Rincon, O. Sierra, J. Petit, and G. Ordoñez, "Control of active and reactive powers in three phase inverters for grid-tied photovoltaic systems under unbalanced voltages", International Conference on Renewable Energy Research and Application (ICRERA),pp. 583-588, Oct. 2014.

[10] G. Caceres, J. Lizarazo, M. Mantilla, and J. Petit, "Active power filters: A comparative analysis of current control techniques", IEEE Andean Regional Conference (ANDESCOM), pp. 1-6, Sept. 2010.

[11] H. Cao, H. Zhang, W. Jiang, and S. Wei, "Research on PQ Control Strategy for PV Inverter in the Unbalanced Grid", Power and Energy Engineering Conference (APPEEC), pp. 1-3, March 2012.

[12] F. Blaabjerg, R. Teodorescu, M. Liserre, and A. Timbus, "Overview of Control and Grid Synchronization for Distributed Power Generation Systems",IEEE Transactions on Industrial Electronics, vol. 53,No. 5, pp. 1398-1409, Oct. 2006.

[13] J. Petit, "Control de filtros activos de potencia para la mitigacion de armonicos y mejora del factor de potencia en sistemas desequilibrados," Universidad Carlos III de Madrid, Ph.D. dissertation, 2007.

[14] H. Akagi, E. Watanabe, and M. Aredes, Instantaneous Power Theory and Applications to Power Conditioning, 1st ed, vol. 6, IEEE Press Editorial Board, 2008, pp. 41-104.

[15] H. Kim and H. Akagi, "The instantaneous power theory on the rotating p-q-r reference frames", Power Electronics and Drive Systems, vol. 1, pp. 422-427, 1999.

[16] I. Diaz, H. Ortiz, M. Mantilla, and J. Petit, "Electrical signals parameter estimation using adaptive filtering: A comparative study",IEEE/PES IEEE Transmission & Distribution Conference and Exposition: Latin America, pp. 745 - 750,Nov. 2010.

[17] J. Kwon, B. Kwon, and K. Nam, "Three-Phase Photovoltaic System With Three-Level Boosting MPPT Control",IEEE Transactions on Power Electronics, vol. 23, No. 5, pp. 2319-2327, Sept. 2008.